

# Thermal Properties of Dry Mixtures of Mine Tailings 1 and Tire Crumbs

Joon Kyu Lee and Julie Q. Shang

**The University of Western Ontario**  
Department of Civil and Environmental Engineering Faculty of Engineering Science





## 1 **Introduction**

2 In geotechnical engineering practice, geomaterials, including natural soil, crushed rock and tailings from  
3 mining activities, and cement concrete, are commonly used as fills of earthworks. On the other hand,  
4 waste and by-product materials such as scrap tire, coal fly/bottom ash, sewage sludge ash, rice husk ash,  
5 etc, are often applied to enhance the physical and chemical properties of the fill materials. These materials  
6 are often required to have specific thermal properties depending on their applications. For instance, good  
7 insulating fills are needed for oil and gas pipelines and underground storage tanks of liquefied natural gas  
8 (LNG). In contrast, geothermal heat pumps and high-voltage power cables require fill materials to  
9 dissipate heat readily. Hence, suitable selection of fill materials is very important for energy savings.

10 In the mining industry, substantial mining tailings are generated worldwide after extraction of  
11 valuable metals and minerals from ore body. The mine tailings are the finely ground rocks, and can be  
12 either reactive (generating acid mine drainage, AMD hereafter) or non-reactive, depending on the  
13 mineralogical composition. Recently, the utilization of mine wastes by modifying the physical and  
14 chemical properties of mine tailings has been practiced, for example, as the backfill of cemented tailings  
15 (Ercikdi et al. 2010) and as the raw material of building bricks (Yellishetty et al. 2008). These  
16 applications have advantages from technical, economic and environmental perspectives. Nevertheless,  
17 most mine tailings have traditionally been disposed on site in the form of impoundments. The surface  
18 impoundments of high water content tailings allow for their consolidation and desiccation. The  
19 impoundments may be in water or dry, depending on the disposal history and site conditions. Some  
20 tailings may be applied as construction materials on the mine site for infrastructures when natural soils are  
21 not available in ample quantity near the site and underwater disposal is not essential to control AMD  
22 (Bussiere 2007). Moreover, the use of such mine tailings can be beneficial for the reduction in tailings  
23 accumulation and costs associated with constructing and reclaiming tailings dykes and other  
24 infrastructures on the mine site.

1 More than one billion scrap tires are produced each year worldwide, and the handling of these scrap  
2 tires has become a serious environment problem over past decades. As a possible alternative for their  
3 disposal, the scrap tires are used in civil engineering applications. The scrap tires are usually grinded to  
4 particles. According to ASTM D 6270 (ASTM 2008), they are classified into three distinct groups in  
5 particle sizes: tire shreds (50 to 305 mm), tire chips (12 to 50 mm) and particulate rubber (less than 12  
6 mm), often known as tire crumbs (Edinçliler et al. 2010). The rubber tire particles are lightweight and  
7 durable, and display favorable drainage characteristic, good thermal insulation and high energy absorption.  
8 They are also comparatively cost effective when used as fills compared to other materials. Owing to these  
9 advantages, tire particles can be applied alone or mixed with other geomaterials as backfills of  
10 embankments, retaining walls, bridge abutments, leachate collection layers in landfills, subgrade thermal  
11 insulators and vibration attenuation media (Humphrey et al. 1997; Tweedie et al. 1998; Aydilek et al.  
12 2006; Tandon et al. 2007; Hazarika et al. 2008).

13 Studies on tire particles and soil-tire particle mixtures have been carried out extensively, including  
14 characterization of mechanical properties such as the strength, compressibility, compactivity and  
15 permeability, as related to the size and shape of tire particles, soil type and mixing ratio (Hudson et al.  
16 2007; Ozkul and Baykal 2007; Wartman et al. 2007; Tanchaisawat et al. 2010; Edinçliler et al. 2010).  
17 Meanwhile, a variety of field and laboratory studies for evaluating toxicity of leachates from scrap tires  
18 have been conducted (Mclsaac and Rowe 2005; Sheehan et al. 2006; Tandon et al. 2007). A  
19 comprehensive overview on the environmental impacts of scrap tires is given in ASTM D 6270 (ASTM  
20 2008). However, the thermal properties of scrap tires and their mixtures with geomaterials, which are  
21 important in the design as insulation fills, have not been addressed in detail in the literature. For instance,  
22 in the work of Humphrey et al. (1997), the thermal conductivity of tire chips was back-calculated by  
23 using one dimensional heat flow theory and measured temperature profile of an in-situ three-layer (soil-  
24 tire chip-soil) system under steady state conditions. Therefore, more information on thermal properties of  
25 tire particles and their mixtures with geomaterials will be beneficial for practical applications.

## 1 **Objective and Scope**

2 This study is directed to the beneficial use of tire particles as lightweight fill materials with improved  
3 thermal insulation. Tailings from a mining site and tire crumbs were selected for the study for reasons  
4 discussed in the previous section. The thermal properties and packing densities of mine tailings mixed  
5 with tire crumbs in dry state were measured to investigate the roles of tire particles inclusion in amending  
6 the thermal and packing behaviors of mineral aggregates. The mixture samples were prepared in the  
7 laboratory by controlling the mixing ratio of the two materials and packing methods. The results of  
8 thermal conductivity and volumetric heat capacity measurements on the mixtures are presented to  
9 demonstrate their correlations with the volumetric mixing ratio of tire crumbs as well as the porosity of  
10 the mixtures.

11 The scope of the study includes a review of concepts from particle packing characteristics relevant to  
12 mixtures of mine tailings and tire crumbs, which will enhance the understanding of the thermal responses  
13 of the mixtures. Methods are addressed to estimate the loosest and densest packing behaviors of the  
14 mixtures from the theory and from experimental investigations, respectively. Based on the experimental  
15 results, a multiple linear regression model for predicting the thermal conductivity of the mixtures is  
16 established as a function of two variables, i.e., the volumetric mixing ratio of tire crumbs and porosity.  
17 The volumetric heat capacity diagram is presented, which enables the volumetric heat capacity to be  
18 determined for the mixtures at known porosity and volumetric mixing ratio of tire crumbs.

## 19 **Heat Transfer in Geomaterials**

20 Heat transfer takes place through conduction, convection and radiation. Of the three mechanisms,  
21 conduction prevails in solids and is the predominant mechanism for heat transfer in most geomaterials  
22 (Farouki 1986). The thermal properties of a geomaterial are affected by the volumetric fractions of its  
23 constituents (air, water, minerals and organic matter). The thermal properties of constituents of  
24 geomaterials vary in a broad range, as shown in Table 1. Furthermore, the fabric of geomaterials, which

1 refers to the arrangement of particles of all size ranges, shapes and associated pores (Mitchell and Soga  
2 2005), has an effect on their thermal properties (Carson et al. 2003; Cote and Konrad 2005).

3 The thermal conductivity  $\lambda$  (W/mK) is defined as the heat flux under a unit temperature gradient  
4 under steady state, one dimensional conditions, as stated in the Fourier's law:

$$5 \quad \lambda = -\frac{q}{dT/dx} \quad (1)$$

6 where  $q$  (W/m<sup>2</sup>) is the heat flux which is the amount of thermal energy transferred per unit time in the  $x$   
7 (m) direction per unit area perpendicular to the transfer direction, and  $T$  (K) is the temperature. A high  
8 thermal conductivity signifies that heat easily propagates through a material. Several researchers (Farouki  
9 1986; Brandon and Mitchell 1989) have pointed out that the thermal conductivity of geomaterials varies  
10 with temperature and pore fluid salinity, as well as the thermal conductivities and volumetric fractions of  
11 constituents.

12 The volumetric heat capacity  $C_v$  (J/m<sup>3</sup>K) is the amount of heat required to change a unit temperature  
13 per unit volume of material:

$$14 \quad C_v = \frac{dQ}{dT} \quad (2)$$

15 where  $Q$  (J/m<sup>3</sup>) is the thermal energy per a unit volume and  $T$  (K) is the temperature. A high volumetric  
16 heat capacity implies that a material has high capacity to store thermal energy. De Vries (1963) suggested  
17 that the volumetric heat capacity of a geomaterial can be estimated as the arithmetic mean of the  
18 volumetric heat capacity  $C_i$  of each constituent in the geomaterial, using the volumetric fraction  $V_i$  as  
19 weight:

$$20 \quad C_v = \sum_i V_i C_i = V_a C_a + V_w C_w + V_s C_s \quad (3)$$

1 where  $C$  and  $V$  denote the volumetric heat capacity and volumetric fraction of each constituent: air ( $a$ ),  
 2 water ( $w$ ), and soil solid ( $s$ ), respectively. Note that the solid constituents include various minerals and  
 3 organic matter, which are not separated. When a dry mixture of mine tailings and tire crumbs is  
 4 considered, Eq. (3) can be rewritten as

$$5 \quad C_v = V_a C_a + V_m C_m + V_t C_t \quad (4)$$

6 where  $C_m$  and  $C_t$  are the volumetric heat capacities, and  $V_m$  and  $V_t$  are the volumetric fractions of mine  
 7 tailings and tire crumbs, respectively. Eq. (4) can be expressed in terms of the porosity and volumetric  
 8 mixing ratio of tire crumbs in the mixture  $R_{mV}$ :

$$9 \quad C_v = n C_a + (1-n)(C_m - R_{mV} C_m + R_{mV} C_t) \quad (5)$$

10 where  $n$  is the porosity of the mixture and  $R_{mV}$  is the volumetric mixing ratio of tire crumbs in the  
 11 mixture.

## 12 **Particle Packing Characteristics**

13 The term of packing may be defined as any manner of arrangement of solid units, in which each  
 14 constituent unit is supported and held in place in the Earth's gravitational field by tangent contact with its  
 15 neighbors (Graton and Fraser 1935). The term *packing* is sometimes used interchangeably with the term  
 16 *fabric* that describes the geomaterial particles and aggregates arrangement in soil mechanics. To  
 17 comprehend the packing behaviors of particulate material mixtures, numerous theoretical and  
 18 experimental studies have been performed. In general, the purposes of these studies are to minimize the  
 19 void or maximize the density of the mixtures in ceramic, construction, food and polymer industries. In  
 20 this section, a literature review on particle packing theories is presented in order to interpret the thermal  
 21 behaviors of mine tailings and tire crumbs mixtures.

1 The porosity  $n$ , void ratio  $e$  and bulk unit weight  $\gamma_b$ , which are strongly related to the packing of  
 2 granular materials, are correlated in the volume-weight phase relationships defined in soil mechanics:

$$3 \quad n = \frac{e}{1+e} = 1 - \frac{\gamma_b}{G_s \gamma_w} \quad (6)$$

4 where  $G_s$  is the specific gravity of a mixture and  $\gamma_w$  is the unit weight of water. In addition, the  
 5 arrangement of the packing is indirectly characterized by means of the coordination number  $N$  (defined  
 6 as the average number of contact points that each particle has with surrounding particles).

7 The packings of uniform spheres provide insight for understanding the packing behaviors of granular  
 8 materials. The regular packing arrangements of uniform spheres can be theoretically calculated using  
 9 geometry. The porosity of uniform spheres ranges from a low of 0.260 for cubic packing to a higher of  
 10 0.476 for rhombohedral packing, and the corresponding coordination number is in the range of 6 to 12  
 11 (White and Walton 1937). However, random packings are more realistic to particulate materials.  
 12 McGeary (1961) revealed that for packings of uniform spheres from 41  $\mu\text{m}$  to 3 mm in size, the minimum  
 13 porosity representing dense random packing lies within the range of 0.375 to 0.405. German (1986)  
 14 summarized the reported porosities for randomly packed uniform spheres, and noted that the porosity for  
 15 dense random packing varies from 0.333 to 0.390 with an average of 0.362, whereas the porosity of loose  
 16 random packing of uniform spheres ranges from 0.375 to 0.440 with an average of 0.408. Murphy (1982)  
 17 compiled the coordination number data from the literature and proposed an empirical relationship  
 18 between the coordination number  $N$  and porosity  $n$  in a randomly packed assembly of uniform spheres,  
 19 namely,

$$20 \quad N = 27.03n^2 - 44.54n + 21.80 \quad (7)$$

21 Although this relation holds for  $0.2 \leq n \leq 0.6$ , it is obvious that the decrease in the porosity of random  
 22 sphere packs increases the coordinate number, both being the result of denser packing.



1           The packing of granular materials is controlled by intrinsic factors such as the shape, size and  
2 gradation of particles, as well as by external factors such as the container wall effect and packing method.  
3 These factors, thus, have influences on the thermal properties of the mixtures.

4           Irregular particles tend to form looser packing than equivalent spheres. The porosity of natural sands  
5 with the same average particle size increases with decreasing the roundness and sphericity, resulting in  
6 lower coordinate number as well as lower stiffness (Cho et al. 2006). The greater the surface roughness is,  
7 the lower the packing density (Shinohara 1984). On the other hand, it was observed that the increase in  
8 the porosity with increasing particle irregularity leads to the decrease in the thermal conductivity (Carson  
9 et al. 2003; Yun and Santamarina 2008).

10           Fine particles likely exhibit looser packing than those of coarse particles due to surface effects.  
11 When the particle sizes approach to less than 50  $\mu\text{m}$ , interparticle forces become prominent because of the  
12 increase in the specific surface area of particles (Samley 1970). The factors such as frictional forces and  
13 bridging between fine particles contribute to the formation of loose or honeycomb structures with high  
14 pore space (Lade et al. 1998). Also, cementation between particles causes agglomeration and particles  
15 clusters, yielding high porosity (Fedors and Landel 1979). Norris (1977) pointed out that finer sands are  
16 generally more irregular and as a result, have higher porosity than coarse sands. Normally, the porosity of  
17 coarse-grained soils is within the range of 0.23 to 0.50, while fine-grained soils can have porosities  
18 greater than 0.50 (Budhu 2007). Meanwhile, it was shown that the thermal conductivity decreases as soil  
19 particles decrease in size (Tavman 1996; Smits et al. 2010).

20           Mixtures of non-uniform particles display a tendency to be denser than those of the same sizes since  
21 finer particles may occupy the voids between coarser particles. Panayiotopoulos (1989) noted that the  
22 influence of particle size distribution on packing efficiency is greater than those of particle size and shape.  
23 As the particle size ratio (i.e., the ratio of coarse particle to fine particle) increases, the coordinate number  
24 of coarse particles increases (Suzuki and Oshima 1983). On the other hand, it was found that the thermal

1 conductivity of well-graded soils is greater than that of poor-graded soils (Brandon and Mitchell 1989;  
2 Cote and Konrad 2005).

3 The container wall effect is defined as the packing of particles being disrupted by the smooth wall of  
4 container, which leads to higher porosity near the wall. In a similar manner, the coarse particles dispersed  
5 or isolated within the fine particles may prevent truly random packing of fine particles at the interfaces of  
6 coarse and fine particles. The container wall effect on packing is less pronounced with rough walls and  
7 irregular particles. When the distance from the wall is at least ten times the particle size, the randomness  
8 of particles becomes constant (McGeary 1961). Meanwhile, the densest and loosest random packings are  
9 affected by packing procedures. In other words, the minimum and maximum porosities of a mixture  
10 depend on the methods employed for their determination (Lade et al. 1998), which may be estimated by  
11 procedures declared in ASTM D 4253 and D 4254 (ASTM 2006a, b). Additionally, other methods have  
12 been adopted by some researchers (Messing and Onada 1978; Al-Jarallah and Tons 1981).

13 For a mixture containing particles of two sizes, it can be idealized as a binary mixture, and its  
14 porosity variation against the volumetric mixing ratio of coarse particles to the total solids is illustrated in  
15 Fig. 1, where porosities at  $R_{mV} = 0$  and 1 correspond to random packings of fine and coarse particles,  
16 respectively. The porosity decreases with an increase in the volumetric mixing ratio of coarse particles  
17 until it reaches a threshold value. This threshold value represents an optimal packing for a binary mixture,  
18 which is a point where the behavior of the mixture changes from fine-dominated to coarse-dominated.  
19 The trend is overturned with further increases in the volumetric mixing ratio of coarse particles. When the  
20 particle size ratio approaches infinity, the voids of the coarse particles are larger enough to allow for the  
21 random packing of fine particles, the porosity  $n_{opt}$  and volumetric mixing ratio  $R_{mV-opt}$  at the optimal  
22 packing can be obtained from the following equations, respectively (Lade et al. 1998):

$$23 \quad n_{opt} = n_c n_f \quad (8)$$

$$R_{mV-opt} = 1 - \frac{1}{e_f} \left( \frac{n_f}{1/e_c + n_f/e_f} \right) \quad (9)$$

where  $n$  and  $e$  denote the porosity and void ratio of each particle in mixtures: coarse ( $c$ ) and fine ( $f$ ), respectively. The theoretical packing curve, i.e., the porosity behavior of mixtures  $n_{mix}$  in Fig. 1, is expressed as

$$n_{mix} = \frac{e_f(1 - R_{mV})}{1 + e_f(1 - R_{mV})} \text{ for } R_{mV} \leq R_{mV-opt} \quad (10)$$

$$n_{mix} = \frac{R_{mV}(e_c + 1) - 1}{R_{mV}(e_c + 1)} \text{ for } R_{mV} \geq R_{mV-opt} \quad (11)$$

It is clear from these equations that the optimal packing point in binary mixtures is not unique because it relies on the packing characteristics of the host materials.

## 9 Experimental Study

To study the thermal and packing behaviors of mine tailings, tire crumbs and their mixtures, an experimental program was designed and carried out. A description of materials, apparatus, sample preparation and methodology is provided in this section, followed by discussion of experimental results and statistical analysis.

### 14 *Materials*

The materials used in this study are mine tailings and tire crumbs. Mine tailings were recovered from the Musselwhite mine, a gold mine located 500 km north of Thunder Bay, Ontario, Canada. Tire crumbs were supplied by a tire recycling facility located in Ontario. The index properties of two materials were determined following the recommended procedures by American Society of Testing and Materials (ASTM), and summarized in Table 2.

1 The specific gravity of mine tailings is 3.37, which is greater than that of typical soils owing to  
 2 predominant amphibole minerals of high specific gravity (Wang et al. 2006), and the specific gravity of  
 3 tire crumbs is measured as 1.19, which is comparable to those reported in ASTM D 6270 (ASTM 2008).  
 4 The Atterberg limit tests on tailings particles finer than 75  $\mu\text{m}$  revealed that the mine tailings are non-  
 5 plastic. Scanning electron microscope (SEM) images of mine tailings and tire crumbs are displayed in Fig.  
 6 2. For mine tailings (Fig. 2(a)), particles are angular to subangular in shape, and typically consist of large  
 7 bulky particles, platy particles and flocks (agglomeration of clay-sized particles). As shown in Fig. 2(b),  
 8 the tire crumbs are angulated and roughened as they are produced through the mill process.

9 The particle size distributions of the mine tailings and tire crumbs are shown in Fig. 3. In Fig. 3(a),  
 10 the shaded area indicates the typical grading of Canadian hard rock tailings as presented by Bussiere  
 11 (2007). The mine tailings are made up of a wide range (0.42 to 138  $\mu\text{m}$ ) of particle sizes, characterized as  
 12 a silt, with 9.4% sand, 83.2% silt and 7.4% clay ( $< 2 \mu\text{m}$ ) sized particles. The size of tire crumbs ranges  
 13 from 0.069 mm to 0.85 mm, as shown in Fig. 3(b). On the other hand, the textures of both the mine  
 14 tailings and tire crumbs are quantified as the effective  $D_{10}$  and median  $D_{50}$  particle sizes, together with  
 15 the coefficient of uniformity  $C_u$  and the coefficient of curvature  $C_c$ , as given in Table 2. Their textures  
 16 can be further specified by using other statistical measures such as mode  $D_m$ , mean  $\bar{D}$ , standard deviation  
 17  $\sigma$ , skewness  $Sk$  and kurtosis  $K$  (see Appendix for the definition and statistical meaning of the measures)  
 18 that are used to characterize the properties of geomaterials. As an example, Carrier (2003) pointed out that  
 19 the  $\bar{D}$  size of particles best represents the particle size for the estimation of the coefficient of permeability  
 20 of a soil than the  $D_{10}$  size of particle. It is also noteworthy that the  $D_{50}$  almost never displays the same  
 21 value as the  $\bar{D}$  since the particle size probability density functions are likely to be skewed. Accordingly,  
 22 the statistical measures of the mine tailings and tire crumbs were computed and are listed in Table 3.  
 23 Based on the descriptive terminology of shapes suggested by Blott and Pye (2001), the mine tailings are  
 24 poorly sorted ( $\sigma = 3.596$ ), with fine skewed (indicating an excess of fines,  $Sk = -0.981$ ) and mesokurtic

1 ( $K = 3.469$ ) distribution, whereas tire crumbs is moderately well sorted ( $\sigma = 1.557$ ), with fine skewed  
2 ( $Sk = -1.043$ ) and leptokurtic ( $K = 3.810$ ) distribution, as comparing to the log-normal distribution. As  
3 shown in Fig. 3(a), meanwhile, the particle size distribution of mine tailings used is characterized as the  
4 tertiary mode, which is attributed to the fact that ore has been artificially ground to a targeted particle size  
5 for liberating gold from the rock.

6 Wang et al. (2006) have studied the mineralogical and geochemical properties of the mine tailings  
7 used in this study. According to their results, the mine tailings contain 3% reactive minerals (i.e.,  
8 pyrrhotite) and the remainder is composed of amphibole, quartz, mica or illite, and chlorite. The amount  
9 of pyrrhotite is small, comparing to that of other sulphide-containing mine tailings reported in the  
10 literature (e.g., 80% pyrrhotite: Amaratunga 1995; 49% pyrite: Ercikdi et al. 2010). This means that the  
11 mine tailings tested has low reactivity. Moreover, the mine tailings contain 1.2% carbonate, in the form of  
12 calcite and dolomite, which provide a pH buffer capacity. On the other hand, the pH of the mine tailings  
13 is measured as 8.4, which is slightly alkaline. This is mainly due to the addition of lime during the milling  
14 process and the presence of carbonates. Up to date, AMD has not been generated on the mine site.

### 15 *Apparatus*

16 In this study, all measurements of thermal properties were conducted using a thermal property analyzer  
17 (Model KD2 Pro, Decagon Devices Inc.). The methodology of the measurement is based on the transient  
18 line heat source theory (Bristow et al. 1998). This apparatus reproduces thermal properties of reference  
19 materials with  $\pm 5\%$  accuracy within the temperature range of - 50 to 150 °C. The KD2 Pro analyzer  
20 comprises a hand-held unit and a sensor. The sensor has two-parallel probes of 1.3 mm diameter and 30  
21 mm length at a spacing of 6 mm, which is inserted into the sample under testing. One of probes contains a  
22 heater and the other, a thermistor. A heat pulse is applied to the heater and, the temperature is  
23 simultaneously recorded at the thermistor. The thermal properties of the sample are automatically

1 determined from the temperature response with time. A single measurement takes about 2 minutes  
 2 including the temperature equilibrium period prior to heating and cooling.

### 3 ***Sample Preparation***

4 In this study, samples tested include mine tailings, tire crumbs, and seven mixtures of the tailings and tire  
 5 particles. The thermal conductivity and volumetric heat capacity of mixtures were measured and  
 6 compared with those of pure mine tailings and pure tire crumbs. Nine samples with the rubber-to-tailings  
 7 weight ratios of 0.0, 0.1, 0.2, 0.3, 0.4, 0.5, 0.6, 0.8 and 1.0 were prepared. The weight ratio was used  
 8 instead of the volumetric ratio, because preparing samples is more readily performed using weight  
 9 measurement. The weight mixing ratios were converted to the volumetric mixing ratios for evaluating  
 10 packing and thermal behaviors of the samples in the analysis related to the volumetric terms. The  
 11 volumetric mixing ratio of tire crumbs in the mixture  $R_{mV}$  can be calculated from the weight mixing ratio  
 12  $R_{mW}$ , knowing the specific gravities of tire crumbs  $G_{st}$ , and mine tailings  $G_{sm}$ , by using the following  
 13 equation (Youwai and Bergado 2003):

$$14 \quad R_{mV} = \frac{R_{mW}}{G_{st}} \left( \frac{1 - R_{mW}}{G_{sm}} + \frac{R_{mW}}{G_{st}} \right)^{-1} \quad (12)$$

15 It is intuitively recognized that the mixtures will form different fabrics under different particle sizes and  
 16 shapes, which will influence the thermal properties of the mixtures, as discussed in the previous section.

### 17 ***Methodology***

18 The tire crumbs and tailings at predetermined weight ratio were placed in a mechanical mixer and mixed  
 19 until the samples were visually homogenous. The mixture was then packed following three different  
 20 procedures: loosest packing, intermediate packing and densest packing. A standard Proctor mold of  
 21 volume 943.7 cm<sup>3</sup> (101.6 mm diameter and 116.4 mm height), as described in ASTM D 698 (ASTM

1 2007), was used as the container. No surcharge and compaction were applied in the sample preparation to  
2 avoid crushing tailings particles and compression of tire particles.

3 A mixture with loosest random packing was achieved following the Method A specified by ASTM  
4 D 4254 standard (ASTM 2006b), in which a funnel was used to pour the mixture into the container. A  
5 mixture with the densest random packing was attained using an electromagnetic vibrating table (Model  
6 VP-51-D1, FMC tech.). A mixture with the intermediate packing was prepared following the same  
7 procedures for the densest packing, but the time and amplitude of vibration were attenuated. For each  
8 rubber-tailings weight ratio, one to three samples were prepared with various degrees of intermediate  
9 packing.

10 After packing, the extension collar on the mold was removed and the excess material was carefully  
11 trimmed off. The weight of the sample was measured for calculation of the bulk unit weight and porosity  
12 from Eq. (6). Lastly, the volumetric fractions of constituents in the sample (air, mine tailings and tire  
13 crumbs) were computed using Eq. (12) with the known porosity.

14 After the sample was prepared and its properties were measured, the KD2 Pro analyzer was  
15 vertically inserted into the sample. A total of three measurements, taken from 50 mm from the mold wall,  
16 were made and the average value and standard deviation were calculated. All measurements were carried  
17 out at the room temperature of 20 °C, with deviation less than  $\pm 0.5$  °C.

## 18 **Results and Discussion**

19 A summary of results for all samples tested is tabulated in Table 4. One can notice that the measured bulk  
20 unit weight and porosity already capture the effects of the particle sizes, shapes and gradation as well as  
21 the container wall effect. In this section, the experiment results are presented and discussed to highlight  
22 the roles of coarse-gained tire particles inclusion in modifying the thermal and packing characteristics of  
23 fine-grained tailings.

## 1 ***Packing Behaviors of Mixtures***

2 The minimum and maximum bulk unit weights ( $\gamma_{\min}$  and  $\gamma_{\max}$ ) of the mixtures are plotted against the  
3 volumetric mixing ratio of tire crumbs, as shown in Fig. 4, in which the bulk unit weights corresponding  
4 to samples with intermediate packing are not included. The variation of the maximum bulk unit weight  
5 with the volumetric mixing ratio of the lightweight tire crumbs is greater than that of the minimum bulk  
6 unit weight. On the other hand, the results indicate that the inclusion of the lightweight tire crumbs  
7 decreases the bulk unit weight regardless of the packing density, and the trend is non-linear, which is due  
8 to the change in the amount of air-entrainment as influenced by the volume of tire crumbs in the mixture.

9 The minimum and maximum porosities ( $n_{\min}$  and  $n_{\max}$ ) of the mixtures against the volumetric  
10 mixing ratio of tire crumbs are shown in Fig. 5, to compare with bulk unit weights in Fig. 4. Again, the  
11 porosities corresponding to intermediate packing are not presented in this plot. The porosity change in Fig.  
12 5 represents the changes of air fraction in mixtures. The porosity of the mixtures decreases as packing  
13 density increases, while the variations of porosity are similar irrespective of packing states. As the  
14 volumetric mixing ratio of tire crumbs increases from 0 to 0.55, both the minimum and maximum  
15 porosities of the mixtures decrease gradually. As the volumetric mixing ratio of tire crumbs further  
16 increase from 0.55 to 1, the limit porosities of the mixtures increase significantly. This trend supports the  
17 fact that the decrease in the bulk unit weight of the mixtures with the increased portion of tire crumbs is  
18 caused not only by the reduced mixture weight, but also by the changes in entrained air in the mixture.  
19 The porosity of mine tailings ranges from 0.44 to 0.60, which is in the range of typical fine-grained soils,  
20 whereas the porosity of tire crumbs varies from 0.63 to 0.68, which are relatively large comparing to  
21 geomaterials. This may be attributed to the angular shape and rough surface of the tire particles. The  
22 observation shows the evidence that the porosity of materials is associated with the combined effect of  
23 particle size, shape and gradation.



1        The binary packing theory, modeled as Eqs. (8)-(11), is applied to the measured porosities of the  
 2 mixtures of mine tailings and tire crumbs, as shown in Fig. 5. Based on particle size statistics of the two  
 3 materials given in Table 3, the particle size ratios of the mode  $D_{m_t} / D_{m_m}$  and the median  $D_{50_t} / D_{50_m}$   
 4 (where the subscript  $t$  and  $m$  denote the tire crumbs and mine tailings, respectively) are computed to be  
 5 9.3 and 17.5, respectively. In addition, the particle size ratio of the mean with standard deviation  
 6  $(\bar{D}_t \pm \sigma_t) / (\bar{D}_m \pm \sigma_m)$  is determined to be between about 20 and 30. The results demonstrate that the fitted  
 7 curves of measured porosities are consistent with the theoretical packing curves: the porosity of the  
 8 mixtures is less than the porosities of pure materials. However, the optimal packings of two limit  
 9 porosities, i.e., minimum and maximum porosities, do not exhibit a distinctive point as derived from the  
 10 ideal binary mixture shown in Fig. 1. This is probably due to the fact that for mixtures with tire crumbs  
 11 content less than the optimal packing value, tire particles do not float within the tailings particles matrix  
 12 without the interference of random tailings packs. For mixtures with tire crumbs content higher than the  
 13 optimal packing value, tailings particles could not migrate into the pore space between tire particles  
 14 without frictional resistance that leads to disconnected tire particles. Similar smooth packing trends for  
 15 mixtures containing construction aggregates of two different sizes have been observed in the literature  
 16 (Al-Jarallah and Tons 1981, Lade et al. 1998, Jones et al. 2002). In their works, the median particle size  
 17 ratio is in the range of about 2 to 30. Polito (1999) analyzed the packing for mixtures of 37 sands and 5  
 18 non-plastic silts, and concluded that the volumetric mixing ratio of sands at the optimal packing point was  
 19 within the range of 0.55 to 0.75. In contrast, for the irregular shaped tire crumbs and tailings mixtures, it  
 20 is found that the optimal packing is located at a lower volumetric mixing ratio of tire crumbs, i.e., in the  
 21 range of 0.50 to 0.60.

22        The relationship between the minimum and maximum porosities of the mixtures is shown in Fig. 6.  
 23 The result reveals that the maximum porosity increases with an increase in the minimum porosity. The  
 24 data regression equation has the form of ( $R^2 = 0.85$ )

$$n_{\max} = 0.48 n_{\min} + 0.36 \quad (13)$$

Based on this relation, the packing method used in this study can be employed to prepare mixtures with minimum and maximum porosities. The correlation can also be used to estimate the minimum porosity from the maximum porosity and vice versa, for rubberized geomaterials.

The porosity range, i.e.,  $n_{\max} - n_{\min}$  (or the void ratio range, i.e.,  $e_{\max} - e_{\min}$ ) is used as an index property of granular geomaterials that reflects their fabrics (Cubrinovski and Ishihara 2000). Fig. 7 shows the porosity range versus the volumetric mixing ratio of tire crumbs. The values of  $n_{\max} - n_{\min}$  slightly increases with the increasing volumetric mixing ratio of tire crumbs first, then it begins to decrease noticeably with a further increase in the volumetric mixing ratio, finally it decrease steadily. This indicates that a transition region exists, ranging from  $R_{mV} = 0.55$  to  $0.75$ . In this region, both the mine tailings portion and tire crumbs portion in the mixtures govern the porosity of the mixtures, beyond this range, the mixture fabric transits from a rigid (i.e., a mine tailings supported fabric) to a soft (i.e., a tire crumbs supported fabric) granular skeleton. Meanwhile, it is shown that there is little porosity change in packing of pure tire crumbs, which is expected since the vibration has limited effect on densification of lightweight and highly compressible materials.

These observations can provide insight to the optimal mixing design of geomaterials mixed with recycled tire particles, which represent rigid-soft mixtures. Furthermore, the results suggest that factors such as the particle sizes, shapes and gradation may control the packing characteristics of the mixtures. The effect of these features to the thermal behavior of the mixtures will be discussed in the following section.

### ***Thermal Behaviors of Mixtures***

The relationships between the thermal conductivity and volumetric mixing ratio of tire crumbs for the densest and loosest random packings are shown in Fig. 8. It is no surprise to see that the thermal

1 conductivities of the mixtures with the densest packing are greater than those with the loosest packing, as  
2 the thermal conductivity of solids is higher than that of air. It is of interest to note from Fig. 8 that the  
3 trends of thermal conductivity curves at two different packing states are similar. For the densest packing,  
4 the thermal conductivity values reduce from 0.248 W/mK for mine tailings to 0.080 W/mK for tire  
5 crumbs, while for the loosest packing, the values decrease from 0.140 to 0.073 W/mK. The mixture  
6 containing 65.4% of tire crumbs by volume (40% by weight) has a reduction of thermal conductivity of  
7 about 50% comparing to the mine tailings without the addition of tire crumbs. More importantly, the  
8 thermal conductivities of the two packing states follow a similar trend compared to packing behaviors as  
9 presented in Fig. 4. This finding substantiates the fact that the thermal conductivity of granular  
10 geomaterials is correlated to the inherent thermal properties of constituents as well as the volumetric  
11 fractions of constituents and arrangement of particles in the mixtures.

12 The relationships between the volumetric heat capacity and volumetric mixing ratio of tire crumbs  
13 for the densest and loosest random packings are shown in Fig. 9. The volumetric heat capacity of the  
14 densest packing mixtures is larger than that of the loosest packing mixtures. On the other hand, as the  
15 volumetric mixing ratio of tire crumbs increases, the volumetric heat capacity initially increases slightly  
16 and then dramatically decreases for both packings. It is also noted that the trend of variation of the  
17 volumetric heat capacity versus the volumetric mixing ratio of tire crumbs is similar to that of the porosity  
18 versus the volumetric mixing ratio of tire crumbs, as indicated in Fig. 5. This embodies that the  
19 volumetric heat capacity of the mixtures is more affected by the volumetric fraction of air than by that of  
20 solid phases. This is attributable to the fact that the volumetric heat capacity of air is three orders of  
21 magnitude lower than that of most solids, including tailings and tire particles.

22 Fig. 10 shows the relationships between the thermal conductivity and porosity for all experimental  
23 data tested in this study, including samples with intermediate packings. The thermal conductivity of mine  
24 tailings decreases with increasing porosity and ranges from 0.248 to 0.140 W/mK for porosities between  
25 0.44 and 0.60. Meanwhile, the thermal conductivity of tire crumbs varies from 0.080 to 0.073 W/mK for

1 porosities ranging from 0.63 to 0.68. The measured thermal conductivities of the mixtures of the two  
2 materials are located within the upper and lower bounds with respect to the mine tailings and tire crumbs,  
3 respectively. This plot also shows that as the weight mixing ratio of tire crumbs increases, the thermal  
4 conductivity decreases. Hence, the thermal insulation effect of recycled tire crumbs can be utilized in  
5 engineering applications.

6 The thermal conductivities of dry geomaterials including crushed rocks, gravels, sands, silts and  
7 clays, as related to their porosities have been studied by many researchers (Kersten 1949; Gangadhara  
8 Rao and Singh 1999; Corte et al. 2009). Fig. 11 shows comparison of the measured values of the thermal  
9 conductivity of mine tailings and tire crumbs and those of other materials reported in the literature. The  
10 thermal conductivity of mine tailings is within the typical range of sands and clays, whereas the thermal  
11 conductivity of tire crumbs is lower than that of typical geomaterials. The plot also explains that the  
12 thermal conductivity of geomaterials is sensitive to the fabric as well as the thermal conductivity of their  
13 constituents. For instance, the thermal conductivity of crushed rocks is scattered and differs from that of  
14 natural gravels despite their similar grain sizes ( $\approx 20$  mm).

15 Fig. 12 shows the relationships between the volumetric heat capacity and porosity for all  
16 experimental data obtained in this study. The volumetric heat capacity of the mixtures decreases with  
17 increasing porosity. The volumetric heat capacity of mine tailings ranges from 1.677 to 1.217 MJ/m<sup>3</sup>K for  
18 porosities between 0.44 and 0.60. On the other hand, the thermal conductivity of dry tire crumbs varies  
19 from 0.901 to 0.811 MJ/m<sup>3</sup>K for porosities ranging from 0.63 to 0.68. These two trends are the upper and  
20 lower bounds of the mixtures of mine tailings and tire crumbs, respectively. Fig. 12 also demonstrates that  
21 the rate of volumetric heat capacity changes against the porosity decreases with increasing weight mixing  
22 ratios of tire crumbs in the mixtures.

23 From Figs. 10-12, one may recognize that the thermal properties of mine tailings and tire crumbs  
24 mixtures strongly depend on the packings of the mixtures as represented by porosity. Consequently, the

1 porosity plays a critical role in heat transfer of the dry mixtures, and can be considered to be a secondary  
 2 factor that captures the primary factors, i.e., the particle sizes, shapes and gradation as well as the particle  
 3 characteristics of host materials. Especially, given the mechanism of thermal contacts at the particle-scale,  
 4 the increase in thermal conductivity with decreasing porosity may reflect the improvement of particle  
 5 contacts in the mixtures.

## 6 **Statistical Analysis**

7 In the above section, the results of thermal properties and packing tests were interpreted to explore the  
 8 correlation between thermal and packing behaviors of the mine tailings and crumb tires mixtures. In this  
 9 section, the results of statistical analysis on the average thermal properties in Table 4 are presented and  
 10 discussed.

11 Regression analysis was used for statistical evaluation. The general multiple linear regression model  
 12 can be formulated in the following equation:

$$13 \quad Y = \beta_0 + \beta_1 X_1 + \beta_2 X_2 + \dots + \beta_i X_i + \beta_n X_n + \varepsilon \quad (14)$$

14 where  $\beta_i$  is the regression coefficient,  $X_i$  is the independent variables,  $Y$  is the dependent variable, and  
 15  $\varepsilon$  is a random error term.

16 In this study, the multiple linear regression analyses were performed in two phases: to build a  
 17 prediction model for the thermal conductivity, and to develop an analysis chart for the volumetric heat  
 18 capacity. In the first phase, the multiple linear regression analysis was carried out to establish the  
 19 relationship of the average thermal conductivity of mine tailings, tire crumbs and their mixtures as related  
 20 to the volumetric mixing ratio of tire crumbs  $R_{mV}$  and porosity  $n$ . In the second phase, the volumetric  
 21 heat capacity values of mine tailings and tire crumbs (i.e.,  $C_m$  and  $C_t$ ) were first computed by using  
 22 multiple linear regression analysis (without accounting for intercept term,  $\beta_0$ ) applied to Eq. (4) with

1 other known variables (i.e.,  $C_v$ ,  $C_a$ ,  $V_a$ ,  $V_m$  and  $V_t$ ), and then the calculated values are applied to Eq. (5)  
 2 to produce a volumetric heat capacity diagram of the mixtures as a function of the volumetric mixing ratio  
 3 of tire crumbs  $R_{mV}$  and porosity  $n$ .

#### 4 ***Regression Model for Thermal Conductivity***

5 A multivariate regression model is developed at a significance level of 5% to relate the thermal  
 6 conductivity  $\lambda$ , and the volumetric mixing ratio of tire crumbs  $R_{mV}$  and porosity  $n$ :

$$7 \quad \lambda = 0.368 - 0.079R_{mV} - 0.353n \quad (15)$$

8 Eq. (15) states that the form of the regression model is consistent with the trends of test results observed  
 9 in Fig. 10. That is, the thermal conductivity decreases with increasing volumetric mixing ratio of tire  
 10 crumbs and increasing porosity.

11 The statistical properties from the regression analysis are summarized in Table 5. The coefficient of  
 12 determination  $R^2$  is 0.908, which indicates a strong correlation between the thermal conductivity and the  
 13 two variables (i.e.,  $R_{mV}$  and  $n$ ). However, a large  $R^2$  value does not necessarily guarantee accurate  
 14 prediction, and therefore the  $F$  - value test is also used to assess the regression model. By definition, the  
 15  $F$  - value is the ratio of the mean squares of regression (MSR) and mean squares of error (MSE) if the  
 16 hypothesis of the test is all regression coefficients being zero (Montgomery et al. 2004). When the  $F$  -  
 17 value of the regression model is larger than the critical  $F$  - value that is the upper limit of the  $F$  ratio, the  
 18 model is feasible at a given probability and degree of freedom. The  $F$  - value is calculated to be 182.5,  
 19 much greater than the critical  $F$  - value at the probability of 95%, i.e., 3.3, suggesting that the regression  
 20 model is highly significant.

21 The standard residual of predicted thermal conductivity, defined as  $r_s = r/SE$ , where  $r_s$  = standard  
 22 residual,  $r$  = residuals, and  $SE$  = standard error, is shown in Fig. 13. The  $SE$  of thermal conductivity

1 regression model is 0.014, and the 95% confidence band is  $\pm 2.03$ . This plot demonstrates that the majority  
2 of the standard residuals fall in the 95% confidence bandwidth of 4.05. The standard residuals are evenly  
3 distributed with regard to the predicted values of thermal conductivity, indicating the regression model is  
4 strongly significant for the estimate of thermal conductivity.

5 Additionally, even if the regression model is statistically significant in terms of  $R^2$ ,  $F$ -value and  
6 standard residuals, implying the model is applicable, it does not guarantee that the model is in any way  
7 optimal. It could be, for example, that one variable is dominating the regression equations while another  
8 variable in the equation is irrelevant. Thus, the significance of the regression coefficients of the variables  
9 in the empirical model was examined via Student's  $t$ -test, which is designed to evaluate the hypothesis  
10 of a particular regression coefficient being zero at an arbitrary probability. The significance of any  
11 regression coefficient can be assessed by comparing the  $t$ -statistic of the regression coefficient (defined  
12 as the ratio of the regression coefficient  $\beta_i$ , and its standard error  $SE$ , i.e.,  $|t-stat| = |\beta_i / SE(\beta_i)|$ ) and  
13 the Student's  $t$  distribution. In other words, if the value of  $t$ -statistic for any of the regression  
14 coefficients is less than the Student's  $t$  distribution at the probability of 95%, i.e., 1.69, it can be  
15 concluded that the data do not provide convincing evidence that the coefficient is different from zero. The  
16 results of Student's  $t$  test reveal that the intercept, volumetric mixing ratio of tire crumbs and porosity are  
17 significant at the probability of 95% in the regression model, as shown in Table 5. Comparing to the  
18 values of  $t$ -statistic obtained, the porosity is slightly more significant than the volumetric mixing ratio of  
19 tire crumbs.

20 As a result, the multiple linear regression model to relate the volumetric mixing ratio of tire crumbs  
21  $R_{mV}$  and porosity  $n$  is highly significant as indicated by a series of statistical analyses. A practical  
22 application of the empirical model is to predict the thermal conductivity if the volumetric mixing ratio of  
23 tire crumbs and porosity of a mixture are known. Also, it can be applied to estimate conditions to attain a

1 desired thermal conductivity. Although the model was built with limited data, it provides a viable insight  
2 to the understanding of the thermal conductivity behaviors of rubberized geomaterials in dry condition.

### 3 ***Analysis Chart for Volumetric Heat Capacity***

4 With known volumetric fractions of constituents (i.e., air, mine tailings and tire crumbs) and volumetric  
5 heat capacities of air and mixtures, the volumetric heat capacities of mine tailings and tire crumbs  
6 mixtures were determined by using the multiple linear regression analysis applied to Eq. (4). The  
7 volumetric heat capacity values of the mine tailings and the tire crumbs are found to be 2.889 and 2.461  
8 MJ/m<sup>3</sup>K, respectively. The resulting values of statistical properties are coefficient of determination  $R^2 =$   
9 0.999 with standard error  $SE = 0.033$  and  $F$  - value = 32,829.6. These volumetric heat capacity values  
10 were used to Eq. (5) that correlates the volumetric heat capacity of mixtures  $C_v$ , volumetric mixing ratio  
11 of tire crumbs  $R_{mV}$ , and porosity  $n$ . Fig. 14 shows an analysis chart for estimating the volumetric heat  
12 capacity of mixtures at known porosity and volumetric mixing ratio of tire crumbs. The curves represent  
13 the porosity range of 0.3 - 0.7, as indicated in Fig. 12. The volumetric heat capacity decreases with  
14 increasing volumetric mixing ratio of tire crumbs at a given porosity. Meanwhile, the volumetric heat  
15 capacity decreases with increasing air fraction in mixtures at a given volumetric mixing ratio of tire  
16 crumbs. These trends are consistent with the results shown in Fig. 12. From a practical perspective, the  
17 analysis chart may prove useful for reasonable predictions of the volumetric heat capacity from easily  
18 available mixture properties, i.e., the volumetric mixing ratio of tire crumbs and porosity only.

### 19 **Summary and Conclusions**

20 The objective of this study was to investigate the thermal and packing behaviors of mine tailings and tire  
21 crumbs mixtures, which has potential applications in utilizing recycled tire particles as lightweight fill  
22 materials with enhanced thermal insulation. The study included a detailed literature review on particle  
23 packing characteristics of spherical and granular materials, which serves to improve the understanding of



1 the packing of mine tailings and tire crumbs mixtures that associate with their thermal properties. In the  
2 experimental program, the thermal and packing properties of dry mixtures of mine tailings and tire  
3 crumbs with different mixing ratios were measured to investigate the roles of tire particles inclusion on  
4 the thermal and packing behaviors of mineral aggregates, as well as to examine their relationships with  
5 the porosity. The following conclusions can be made based on the results of this study:

- 6 1. The factors affecting the packing and thermal properties of geomaterials include the particle size,  
7 shape and gradation as well as the container wall effect and packing method.
- 8 2. The bulk unit weights of the loosest and densest packed mixtures decreased non-linearly with  
9 increasing volumetric mixing ratios of tire crumbs in the mixtures, and the variations of their thermal  
10 conductivities were similar to the convex-shaped variations of bulk unit weights.
- 11 3. The minimum and maximum porosities of the mixtures against the volumetric mixing ratio of tire  
12 crumbs showed the smooth concave-shaped variation, not the sharp V-shaped variation derived from  
13 the ideal binary mixture. As increased the volumetric mixing ratios of tire crumbs in the mixtures, the  
14 volumetric heat capacity values of the mixtures corresponding to the densest and loosest packings  
15 initially increased slightly and then decreased considerably, similar to the trend of porosity variation.
- 16 4. At the volumetric mixing ratios of tire crumbs of 0.55 to 0.75, the mixtures demonstrated transitional  
17 fabrics, i.e., the structure changed from a tailings controlled rigid fabric and a rubber particles  
18 controlled soft fabric.
- 19 5. The porosity plays a preponderant role in heat transfer of the dry mixtures: both the thermal  
20 conductivity and the volumetric heat capacity increased linearly with decreasing porosity.
- 21 6. A multiple linear regression model was developed to estimate the thermal conductivity of the mine  
22 tailings and tire crumbs mixtures as related to the volumetric mixing ratio of tire crumbs and porosity.  
23 A series of statistical analyses revealed that the regression model is highly significant.

1 7. An analysis chart was established that enables the volumetric heat capacity of the mine tailings and  
 2 tire crumbs mixtures to be determined at the known porosity and volumetric mixing ratio of tire  
 3 crumbs in the mixtures.

4 It is believed that the findings and interpretation methods presented in this study will be beneficial for the  
 5 understanding of the thermal characteristics of rubberized geomaterials in dry condition.

## 6 **Acknowledgements**

7 The authors acknowledge the support provided by the National Science and Engineering Research  
 8 Council of Canada (NSERC). The contribution of Goldcrop Musselwhite Mine and Ideal Rubber  
 9 Industries Corporation for providing test materials is also highly appreciated.

## 10 **Appendix**

11 The statistical measures, i.e., mode  $D_m$ , mean  $\bar{D}$ , standard deviation  $\sigma$ , skewness  $Sk$  and kurtosis  $K$ ,  
 12 can be used to demonstrate a particle size distribution characteristics, which is described succinctly by  
 13 Blott and Pye (2001): those quantifying the size with the highest frequency; the average size; the spread  
 14 (sorting) of the size around the average; the symmetry or preferential spread (skewness) to one side of the  
 15 average; and the degree of concentration of the particles relative to the average (kurtosis). These measures  
 16 are commonly calculated geometrically (based on log-normal distribution) using moment method, which  
 17 are defined as follows:

$$18 \quad \bar{D} = \exp \sum f \ln D \quad (16)$$

$$19 \quad \sigma = \exp \sqrt{\sum f (\ln D - \ln \bar{D})^2} \quad (17)$$

$$20 \quad Sk = \frac{\sum f (\ln D - \ln \bar{D})^3}{\ln \sigma^3} \quad (18)$$

$$K = \frac{\sum f (\ln D - \ln \bar{D})^4}{\ln \sigma^4} \quad (19)$$

where  $f$  is the fraction of particles between two sieve sizes and  $D$  is the average particle size between two sieve sizes.

#### References

- Al-Jarallah, M., and Tons, E. (1981). "Void content prediction in two-size aggregate mixes." *Journal of Testing and Evaluation*, 9(1), 3-10.
- Amaratunga, L.M. (1995). "Cold-bond agglomeration of reactive pyrrhotite tailings for backfill using low cost binders: Gypsum  $\beta$ -Hemihydrate and cement." *Minerals Engineering*, 8(12), 1455-1465.
- ASTM. (2006a). "Standard test methods for maximum index density and unit weight of soils using a vibration table" *D4253-06*, West Conshohocken, Pa.
- ASTM. (2006b). "Standard test methods for minimum index density and unit weight of soils and calculation of relative density." *D4254-06*, West Conshohocken, Pa.
- ASTM. (2007). "Standard test methods for laboratory compaction characteristics of soil using standard effort [12,400 ft-lb/ft<sup>3</sup> (600 kN-m/m<sup>3</sup>)]." *D698-07*, West Conshohocken, Pa.
- ASTM. (2008). "Standard practice for use of scrap tires in civil engineering applications." *D6270-08*, West Conshohocken, Pa.
- Aydilek, A.H., Madden, E.T., and Demirkan, M.M. (2006). "Field evaluation of a leachate collection system constructed with scrap tires." *Journal of Geotechnical and Geoenvironmental Engineering*, 132(8), 990-1000.
- Balland, V., and Arp, P.A. (2005). "Modelling soil thermal conductivities over a wide range of conditions." *Journal of Environmental Engineering Science*, 4(6), 549-558.
- Blott, S.J., and Pye, K. (2001). "GRADISTAT: a grain size distribution and statistics package for the analysis of unconsolidated sediments." *Earth Surface Processes and Landforms*, 26(11), 1237-1248.
- Brandon, T.L., and Mitchell, J.K. (1989). "Factors influencing thermal resistivity of sands." *Journal of Geotechnical Engineering*, 115(12), 1683-1698.

- 1 Bristow, K.L. (1998). "Measurement of thermal properties and water content of unsaturated sandy soil  
2 using dual-probe heat-pulse probes." *Agricultural and Forest Meteorology*, 89(2), 75-84.
- 3 Budhu, M. (2007). *Soil mechanics and foundations*, 2nd ed., John Wiley & Sons, New Jersey.
- 4 Bussiere, B. (2007). "Colloquium 2004: hydrogeotechnical properties of hard rock tailings from metal  
5 mines and emerging geoenvironmental disposal approaches." *Canadian Geotechnical Journal*, 44(9),  
6 1019-1052.
- 7 Carrier III, W.D. (2003). "Goodbye, Hazen; hello, Kozeny-Carman." *Journal of Geotechnical and  
8 Geoenvironmental Engineering*, 129(11), 1054-1056.
- 9 Carson, J.K., Lovatt, S.J., Tanner, D.J., and Cleland, A.C. (2003). "An analysis of the influence of  
10 material structure on the effective thermal conductivity of theoretical porous materials using finite  
11 element simulations." *International Journal of Refrigeration*, 26(8), 873-880.
- 12 Cho, G., Dodds, J., and Santamarina, J.C. (2006). "Particle shape effects on packing density, stiffness,  
13 and strength: natural and crushed sands." *Journal of Geotechnical and Geoenvironmental  
14 Engineering*, 132(5), 591-602.
- 15 Cortes, D.D., Martin, A.I., Yun, T.S., Francisca, F.M., Santamarina, J.C., and Ruppel, C. (2009).  
16 "Thermal conductivity of hydrate-bearing sediments." *Journal of Geophysical Research*, 114,  
17 B11103.
- 18 Cote, J., and Konrad, J. (2005). "A generalized thermal conductivity model for soils and construction  
19 materials." *Canadian Geotechnical Journal*, 42(2), 443-458.
- 20 Cubrinovski, M., and Ishihara, K. (2000). "Flow potential of sandy soils with different grain  
21 compositions." *Soils and Foundations*, 40(4), 103-119.
- 22 De Vries, D.A. (1963). "Thermal properties of soils." *Physics of Plant Environment* edited by W.R. van  
23 Wijk, North-Holland Publishing Company, Amsterdam, 210-235.
- 24 Edinçliler, A., Baykal, G., and Saygili, A. (2010). "Influence of different processing techniques on the  
25 mechanical properties of used tires in embankment construction." *Waste Management*, 30(6), 1073-  
26 1080.

- 1 Ercikdi, B., Cihangir, F., Kesimal, A., Deveci, H., and Alp, I. (2010). "Utilization of water-reducing  
2 admixtures in cemented paste backfill of sulphide-rich mill tailings." *Journal of Hazardous*  
3 *Materials*, 179(1-3), 940-946.
- 4 Farouki, O.T. (1986). *Thermal properties of soils*, Series on Rock and Soil Mechanics Vol. 11, Trans  
5 Tech Publications, Clausthal-Zellerfeld.
- 6 Fedors, R.F., and Landel, R.F. (1979). "Effect of surface adsorption and agglomeration on the packing of  
7 particles." *Powder Technology*, 23(2), 219-223.
- 8 Gangadhara Rao, M.V.B.B., and Singh, D.N. (1999). "A generalized relationship to estimate thermal  
9 resistivity of soils." *Canadian Geotechnical Journal*, 36(4), 767-773.
- 10 German, R.M. (1989). *Particle packing characteristics*, Metal Power Industries Federation, Princeton.
- 11 Gratton, L.C., and Fraser, H.J. (1935). "Systematic packing of spheres: with particular relation to porosity  
12 and permeability." *Journal of Geology*, 43(8), 785-909.
- 13 Hazarika, H., Kohama, E., and Sugano, T. (2008). "Underwater shake table tests on waterfront structures  
14 protected with tire chip cushion." *Journal of Geotechnical and Geoenvironmental Engineering*,  
15 134(12), 1706-1719.
- 16 Hudson, A.P., Beavon, R.P., Powrie, W., and Parkes, D. (2007). "Hydraulic conductivity of tyres in  
17 landfill drainage systems." *Proceedings of Institution of Civil Engineers: Waste and Resource*  
18 *Management*, 160(WR2), 63-70.
- 19 Humphrey, D.N., Chen, L.H., and Eaton, R.A. (1997). "Laboratory and field measurement of the thermal  
20 conductivity of tire chips for use as subgrade insulation." *Preprint No. 971289*, Transportation  
21 Research Board, Washington, D.C.
- 22 Jones, M.R., Zheng, L., and Newlands, M.D. (2002). "Comparison of particle packing models for  
23 proportioning concrete constituents for minimum voids ratio." *Materials and Structures*, 35(5), 301-  
24 309.
- 25 Kersten, M.S. (1949). *Laboratory research for the determination of the thermal properties of soils*,  
26 Research Laboratory Investigation. Engineering Experiment Station, Technical Report 23,  
27 University of Minnesota, Minneapolis.

- 1 Krishnaiah, S., and Singh, D.N. (2006). "Determination of thermal properties of some supplementary  
2 cementing materials used in cement and concrete." *Construction and Building Materials*, 20(3), 193-  
3 198.
- 4 Lade, P.V., Liggio, C.D., and Yamamuro, J.A. (1998). "Effects of non-plastic fines on minimum and  
5 maximum void ratios of sand." *Geotechnical Testing Journal*, 21(4), 336-347.
- 6 Madsen, F.T. (1998). "Clay mineralogical investigations related to nuclear waste disposal." *Clay*  
7 *Minerals*, 33(1), 109-129.
- 8 McGeary, R.K. (1961). "Mechanical packing of spherical particles." *Journal of the American Ceramic*  
9 *Society*, 44(10), 513-522.
- 10 Mclsaac, R., and Rowe, R.K. (2005). "Change in leachate chemistry and porosity as leachate permeates  
11 through tire shreds and gravel." *Canadian Geotechnical Journal*, 42(4), 1173-1188.
- 12 Messing, G.L., and Onada, G.Y. (1978). "Inhomogeneity - packing density relations in binary powders -  
13 experimental studies." *Journal of the American Ceramic Society*, 61(7-8), 363-366.
- 14 Midttomme, K., and Roaldset, E. (1998). "The effect of grain size on thermal conductivity of quartz sands  
15 and silts." *Petroleum Geoscience*, 4(2), 165-172.
- 16 Mitchell, J.K., and Soga, K. (2005). *Fundamentals of soil behavior*, 3rd ed., John Wiley & Sons, New  
17 Jersey.
- 18 Montgomery, D.C., Runger, G.C., and Hubele, N.F. (2004). *Engineering statistics*, 3rd ed., John Wiley &  
19 Sons, New York.
- 20 Murphy, W.F. (1982). "Effects of microstructure and pore fluids on the acoustic properties of granular  
21 sedimentary materials." PhD Thesis, Stanford University, Stanford.
- 22 Naidu, A.D., and Singh, D.N. (2004). "Field probe for measuring thermal resistivity of soils." *Journal of*  
23 *Geotechnical and Geoenvironmental Engineering*, 130(2), 213-216.
- 24 Norris, G. (1977). "The drained shear strength of uniform quartz sand as related to particle size and  
25 natural variation in particle shape and surface roughness." PhD Thesis, The University of California,  
26 Berkeley.

- 1 Ould-Lahoucine, C., Sakashita, H., and Kumada, T. (2002). "Measurement of thermal conductivity of  
2 buffer materials and evaluation of existing correlations predicting it." *Nuclear Engineering and*  
3 *Design*, 216(1-3), 1-11.
- 4 Ozkul, Z.H., and Baykal, G. (2007). "Shear behavior of compacted rubber fiber-clay composite in drained  
5 and undrained loading." *Journal of Geotechnical and Geoenvironmental Engineering*, 133(7), 767-  
6 781.
- 7 Panayiotopoulos, K.P. (1989). "Packing of sands - a review." *Soil and Tillage Research*, 13(2), 101-121.
- 8 Polito, C.P. (1999). "The effect of nonplastic and plastic fines on the liquefaction of sandy soils." PhD  
9 Thesis, Virginia Polytechnic Institute and State University, Blacksburg.
- 10 Samlley, I. (1970). "Cohesion of soil particles and the intrinsic resistance of simple soil system to wind  
11 erosion." *European Journal of Soil Science*, 21(1), 154-161.
- 12 Sheehan, P.J., Warmerdam, J.M., Ogle, S., Humphrey, D.N., and Patenaude, S.M. (2006). "Evaluating the  
13 risk to aquatic ecosystems posed by leachate from tire shred fill in road using toxicity tests, toxicity  
14 identification evaluations, and groundwater modeling." *Environmental Toxicology and Chemistry*,  
15 25(2), 400-411.
- 16 Shinohara, K. (1984). "Rheological property of particulate solids." *Handbook of Powder Science and*  
17 *Technology* edited by M.E. Fayed, and L. Otten., Van Nostrand Reinhold Co., New York, 129-169.
- 18 Smits, K.M., Sakaki, T., Limsuway, A., and Illangasekare, T.H. (2010). "Thermal conductivity of sands  
19 under varying moisture and porosity in drainage-wetting cycles." *Vadose Zone Journal*, 9(1), 172-  
20 180.
- 21 Suzuki, M., and Oshima, T. (1983). "Estimation of the co-ordination number in a multi-component  
22 mixture of spheres." *Powder Technology*, 35(2), 159-166.
- 23 Tanchaisawat, T., Bergado, D.T., Voottipruex, P., and Shehzad, K. (2008). "Interaction between geogrid  
24 reinforcement and tire chip-sand lightweight backfill." *Geotextiles and Geomembranes*, 28(1), 119-  
25 127.
- 26 Tandon, V., Velazco, D.A., Nazarian, S., and Picornell, M. (2007). "Performance monitoring of  
27 embankment containing tire chips: case study." *Journal of Performance Constructed Facilities*,  
28 21(3), 207-214.

- 1 Tavman, I.H. (1996). "Effective thermal conductivity of granular porous materials." *International*  
2 *Communication in Heat and Mass Transfer*, 23(2), 169-176.
- 3 Tweedie, J.J., Humphrey, D.N., and Sandford, T.C. (1998). "Tire shreds as lightweight retaining wall  
4 backfill: active condition." *Journal of Geotechnical and Geoenvironmental Engineering*, 124(11),  
5 1061-1070.
- 6 Wang, H.L., Shang, J.Q., Kovac, V., and Ho, K.S. (2006). "Utilization of Atikokan coal fly ash in acid  
7 rock drainage control from Musselwhite Mine tailings." *Canadian Geotechnical Journal*, 43(3), 229-  
8 243.
- 9 Wartman, J., Natale, M.F., and Strenk, P.M. (2007). "Immediate and time-dependent compression of tire  
10 derived aggregate." *Journal of Geotechnical and Geoenvironmental Engineering*, 133(3), 245-256.
- 11 White, H.E., and Walton, S.F. (1937). "Particle packing and particle shape." *Journal of the American*  
12 *Ceramic Society*, 20(1-12), 155-166.
- 13 Yellishetty, M., Karpe, V., Reddy, E.H., Syubhash, K.N., and Ranjith, P.G. (2008). "Reuse of iron ore  
14 mineral wastes in civil engineering constructions: a case study." *Resources, Conservation and*  
15 *Recycling*, 52(11), 1283-1289.
- 16 Youwai, S. and Bergado, D.T. (2003). "Strength and deformation characteristics of shredded rubber tire-  
17 sand mixtures." *Canadian Geotechnical Journal*, 40(2), 254-264.
- 18 Yun, T.S., and Santamarina, J.C. (2008). "Fundamental study of thermal conduction in dry soils."  
19 *Granular Matter*, 10(3), 197-207.
- 20



1 Table 1 Densities and thermal properties of basic geomaterial constituents

Material	Particle density $\rho$ (g/cm <sup>3</sup> )	Thermal conductivity $\lambda$ (W/mK)	Volumetric heat capacity $C_v$ (MJ/m <sup>3</sup> K)
Air	0.00125 <sup>a</sup>	0.025 to 0.026 <sup>a</sup> (283 K)	$1.25 \times 10^{-3}$ <sup>a</sup>
Water	1 <sup>a</sup>	0.57 to 0.58 <sup>a</sup> (283 K)	4.18 <sup>a</sup>
Quartz	2.66 <sup>a,b</sup>	8.8 <sup>a</sup> (283 K)	2.01 <sup>a</sup> 2.13 <sup>b</sup>
Other minerals	2.65 <sup>a,b</sup>	2.0 <sup>a†</sup> (298 K) 3.5 <sup>a‡</sup> (298 K)	2.01 <sup>a</sup> 2.39 <sup>b</sup>
Organic matter	1.3 <sup>a</sup>	0.25 <sup>a</sup> (-)	2.51 <sup>a</sup>

2 †and ‡: values are for feldspar and mica, and amphibolite, respectively.

3 <sup>a</sup> Balland and Arp (2005)4 <sup>b</sup> Bristow (1998)

5

6 Table 2 Index properties of mine tailings and tire crumbs

Properties	Mine tailings	Tire crumbs
Specific gravity, $G_s$	3.374	1.190
Optimum water content, $w_{opt}$ (%)	13.5	-
Maximum dry unit weight, $\gamma_{d\max}$ (kN/m <sup>3</sup> )	19.5	-
Effective size, $D_{10}$ ( $\mu\text{m}$ )	2.8	237.1
Median size, $D_{50}$ ( $\mu\text{m}$ )	25.6	448.1
Coefficient of uniformity, $C_u$	11.43	2.08
Coefficient of curvature, $C_c$	1.61	0.96

7

8

9 Table 3 Particle size statistics of mine tailings and tire crumbs

Sample statistics	Mine tailings	Tire crumbs
Mode, $D_m$ ( $\mu\text{m}$ )	45.7	425.0
Mean, $\bar{D}$ ( $\mu\text{m}$ )	18.5	444.4
Standard deviation, $\sigma$ ( $\mu\text{m}$ )	3.596	1.557
Skewness, $Sk$ ( $\mu\text{m}$ )	-0.981	-1.043
Kurtosis, $K$ ( $\mu\text{m}$ )	3.469	3.810

10

1 Table 4 Summary of packings and thermal properties of the mixtures tested

No.	Weight mixing ratio of tire crumbs $R_{mW}$ (-)	Volumetric mixing ratio of tire crumbs $R_{mV}$ (-)	Bulk unit weight $\gamma_b$ (kN/m <sup>3</sup> )	Porosity $n$ (-)	Thermal conductivity $\lambda$ (W/mK)	Volumetric heat capacity $C_v$ (MJ/m <sup>3</sup> K)
1	0	0	13.3	0.60	0.140 (0.003) <sup>†</sup>	1.217 (0.003) <sup>†</sup>
2	0	0	14.8	0.55	0.166 (0.002)	1.287 (0.008)
3	0	0	16.2	0.51	0.204 (0.003)	1.452 (0.012)
4	0	0	17.1	0.48	0.226 (0.005)	1.574 (0.014)
5	0	0	18.7	0.44	0.248 (0.002)	1.677 (0.029)
6	0.1	0.240	12.8	0.54	0.138 (0.003)	1.259 (0.014)
7	0.1	0.240	13.9	0.50	0.155 (0.002)	1.312 (0.008)
8	0.1	0.240	15.2	0.46	0.189 (0.003)	1.501 (0.007)
9	0.1	0.240	16.8	0.40	0.218 (0.004)	1.617 (0.026)
10	0.1	0.240	17.7	0.37	0.245 (0.003)	1.728 (0.018)
11	0.2	0.415	11.2	0.54	0.127 (0.005)	1.272 (0.041)
12	0.2	0.415	12.5	0.48	0.146 (0.003)	1.362 (0.017)
13	0.2	0.415	13.4	0.45	0.164 (0.005)	1.447 (0.023)
14	0.2	0.415	14.5	0.40	0.186 (0.009)	1.642 (0.036)
15	0.2	0.415	15.4	0.36	0.220 (0.004)	1.731 (0.010)
16	0.3	0.549	10.2	0.52	0.123 (0.002)	1.255 (0.006)
17	0.3	0.549	10.9	0.49	0.139 (0.005)	1.325 (0.014)
18	0.3	0.549	11.9	0.44	0.166 (0.003)	1.491 (0.021)
19	0.3	0.549	12.6	0.41	0.176 (0.004)	1.542 (0.028)
20	0.3	0.549	13.6	0.36	0.209 (0.003)	1.711 (0.012)
21	0.4	0.654	8.7	0.55	0.114 (0.002)	1.181 (0.008)
22	0.4	0.654	9.4	0.51	0.127 (0.002)	1.278 (0.014)
23	0.4	0.654	9.9	0.48	0.131 (0.002)	1.304 (0.017)
24	0.4	0.654	10.4	0.46	0.145 (0.001)	1.397 (0.005)
25	0.4	0.654	11.1	0.42	0.165 (0.008)	1.532 (0.005)
26	0.5	0.739	7.5	0.56	0.113 (0.002)	1.157 (0.017)
27	0.5	0.739	7.8	0.55	0.118 (0.003)	1.191 (0.021)
28	0.5	0.739	8.3	0.52	0.121 (0.002)	1.207 (0.017)
29	0.5	0.739	8.5	0.51	0.131 (0.002)	1.294 (0.008)
30	0.5	0.739	9.1	0.47	0.138 (0.002)	1.354 (0.008)
31	0.6	0.810	6.8	0.57	0.104 (0.003)	1.131 (0.011)
32	0.6	0.810	7.2	0.54	0.110 (0.003)	1.194 (0.007)
33	0.6	0.810	7.6	0.52	0.117 (0.001)	1.240 (0.010)
34	0.6	0.810	8.0	0.49	0.126 (0.003)	1.307 (0.014)
35	0.8	0.919	5.2	0.62	0.089 (0.000)	0.987 (0.006)
36	0.8	0.919	5.6	0.58	0.097 (0.001)	1.061 (0.005)
37	0.8	0.919	6.0	0.55	0.104 (0.002)	1.124 (0.017)
38	1	1	3.8	0.68	0.073 (0.001)	0.811 (0.010)
39	1	1	4.0	0.66	0.076 (0.002)	0.855 (0.016)
40	1	1	4.3	0.63	0.080 (0.001)	0.901 (0.011)

2 <sup>†</sup> Standard deviation

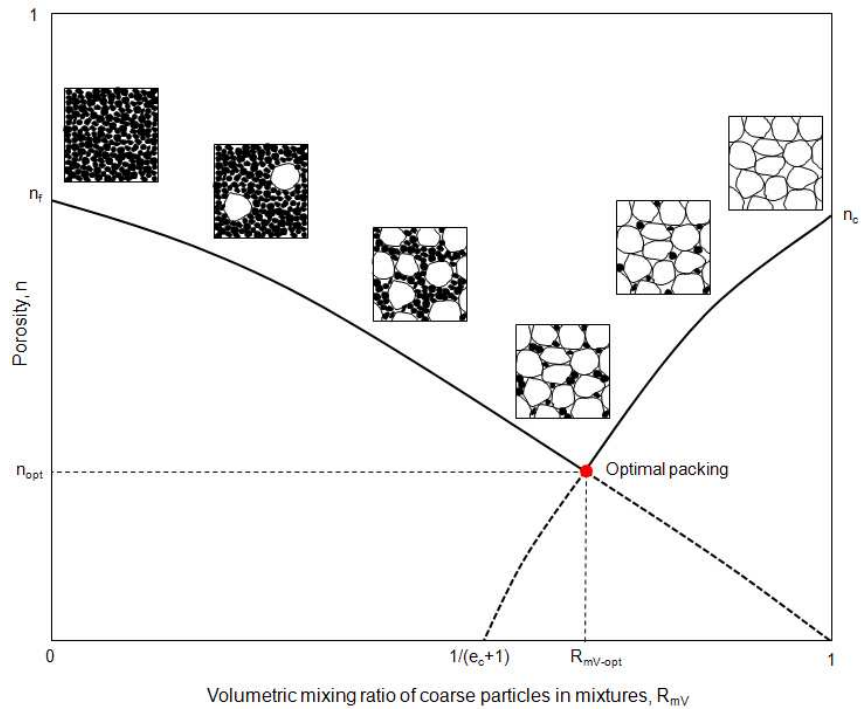
3

1 Table 5 Summary of multiple linear regression analysis result

Observations	40		
$R$ - squared	0.908		
Standard error	0.014		
$F$ - value	182.5		
	Coefficients	Standard error	$t$ - statistic
Intercept	0.368	0.015	24.007
$R_{mV}$	-0.079	0.008	-9.424
$n$	-0.353	0.033	-10.697

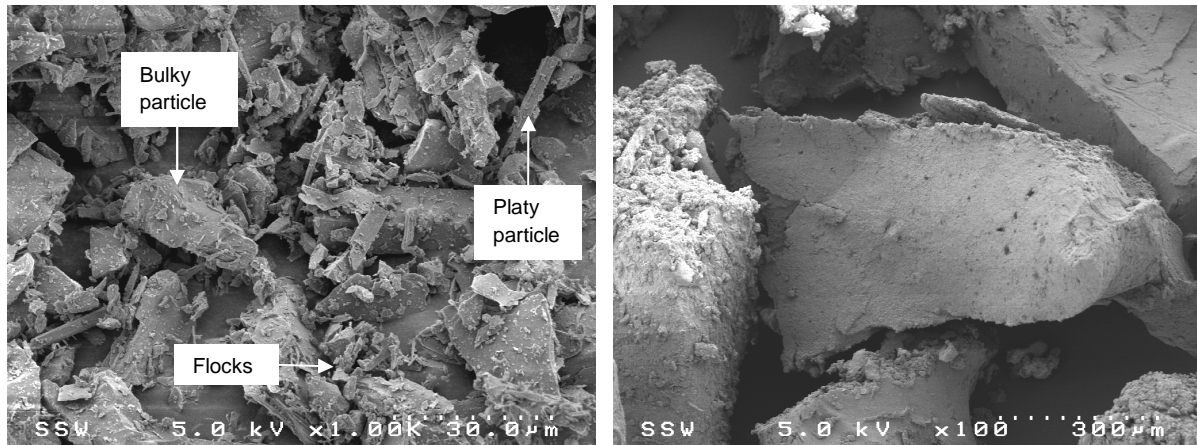
2

3



1  
2  
3  
4  
5

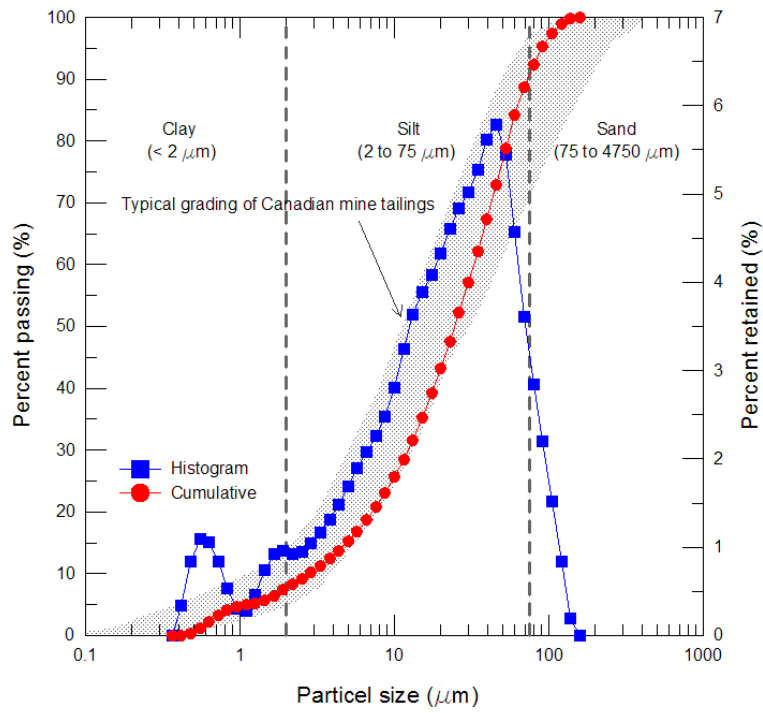
Fig. 1 Porosity in binary packing against volumetric mixing ratio of coarse particles in mixtures (modified from Lade et al. (1998))



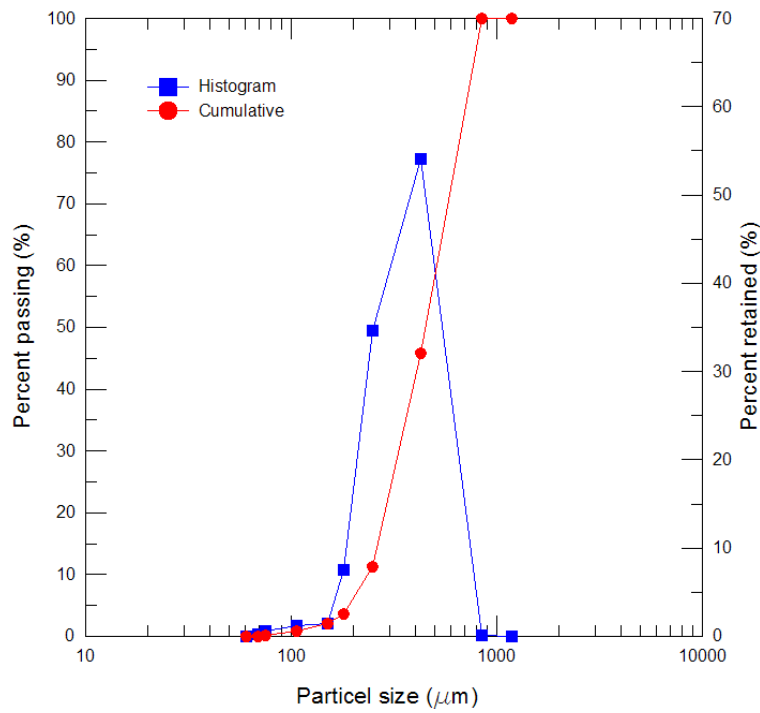
6  
7  
8  
9

(a) (b)

Fig. 2 SEM images: (a) mine tailings; (b) tire crumbs



(a)

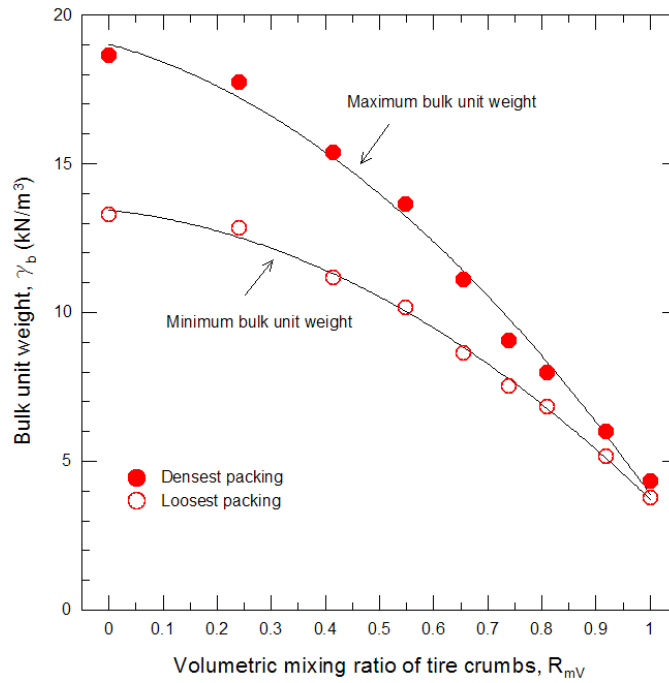


(b)

Fig. 3 Particle size distribution curves: (a) mine tailings; (b) tire crumbs

1  
2

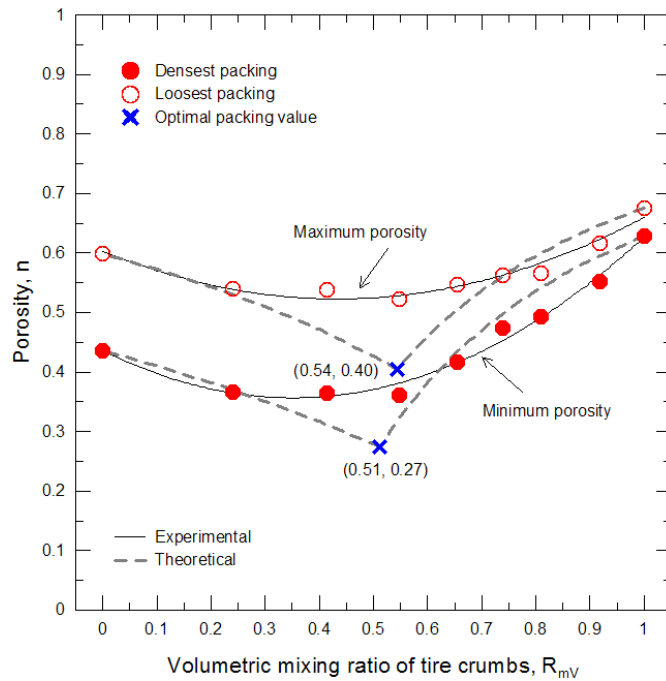
3  
4  
5



1

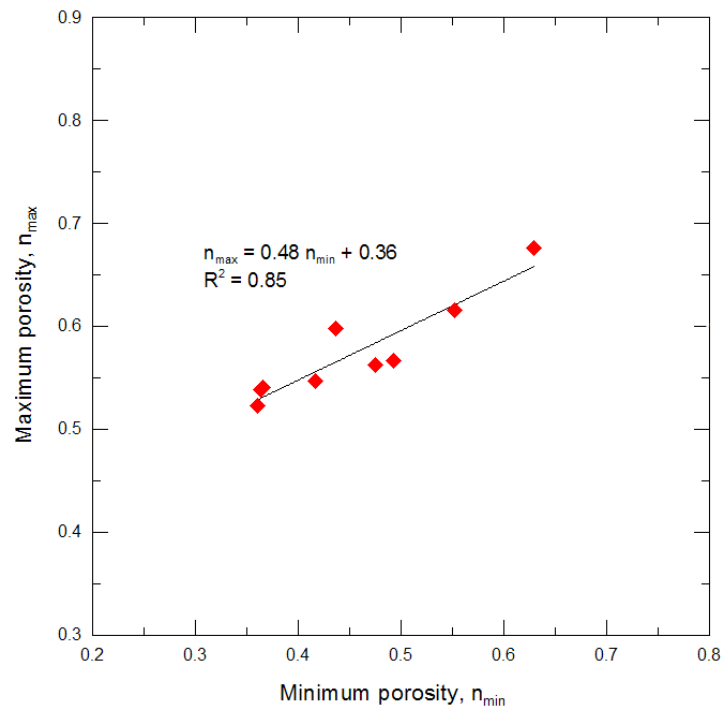
2 Fig. 4 Variations of minimum and maximum bulk unit weights for mixtures of mine tailings and tire  
3 crumbs

4



5

6 Fig. 5 Variations of minimum and maximum porosities for mixtures of mine tailings and tire crumbs

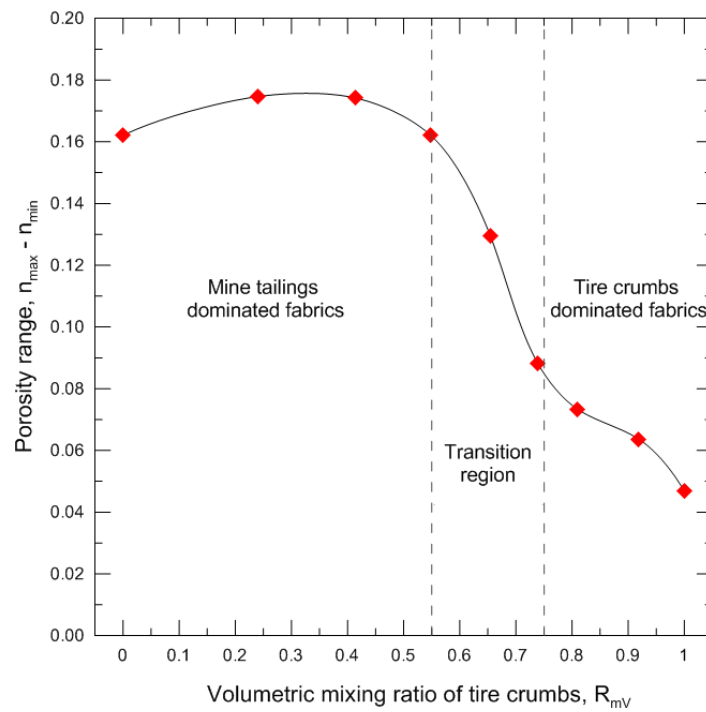


1

2

3

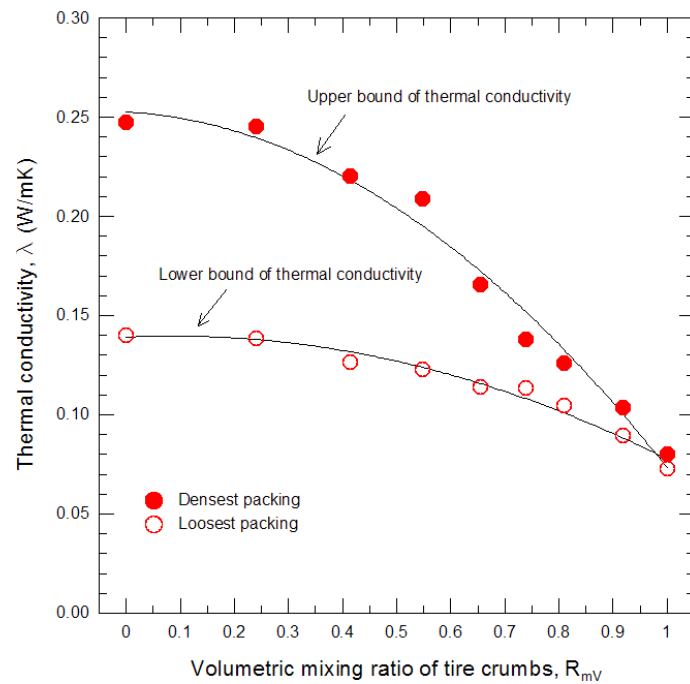
Fig. 6 Correlation between minimum and maximum porosities



4

5

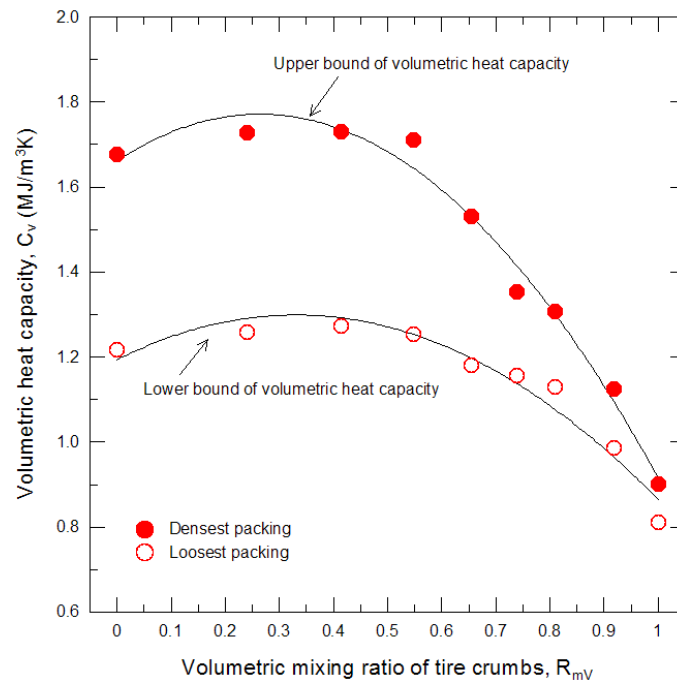
Fig. 7 Change in porosity ranges for mixtures of mine tailings and tire crumbs



1

2 Fig. 8 Relationships between thermal conductivity and volumetric mixing ratio of tire crumbs for loosest  
3 and densest packings for mine tailings and tire crumbs mixtures

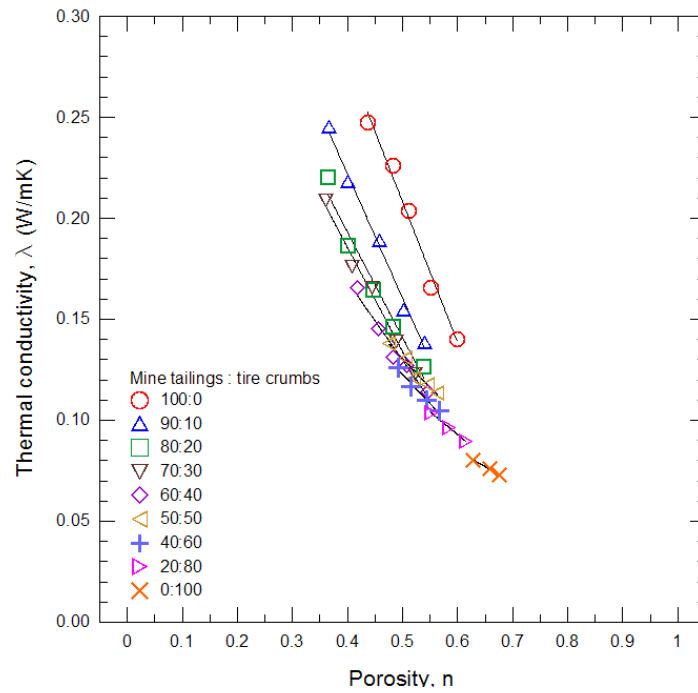
4



5

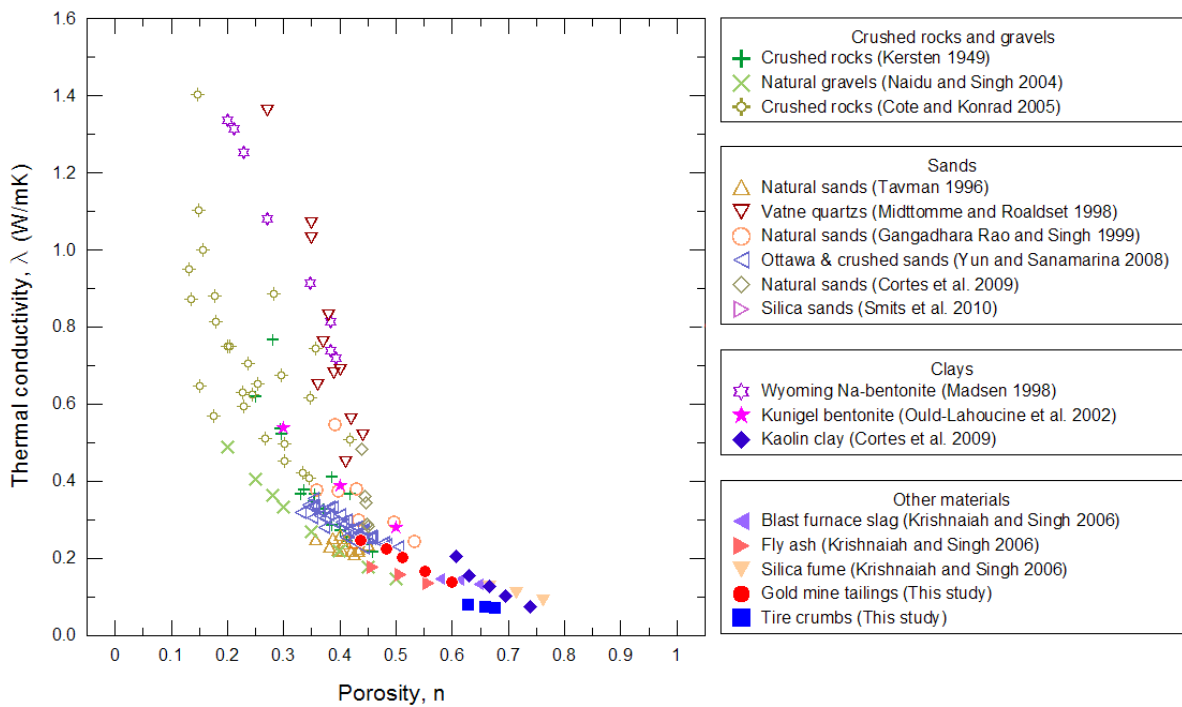
6 Fig. 9 Relationships between volumetric heat capacity and volumetric mixing ratio of tire crumbs for  
7 loosest and densest packings for mine tailings and tire crumbs mixtures





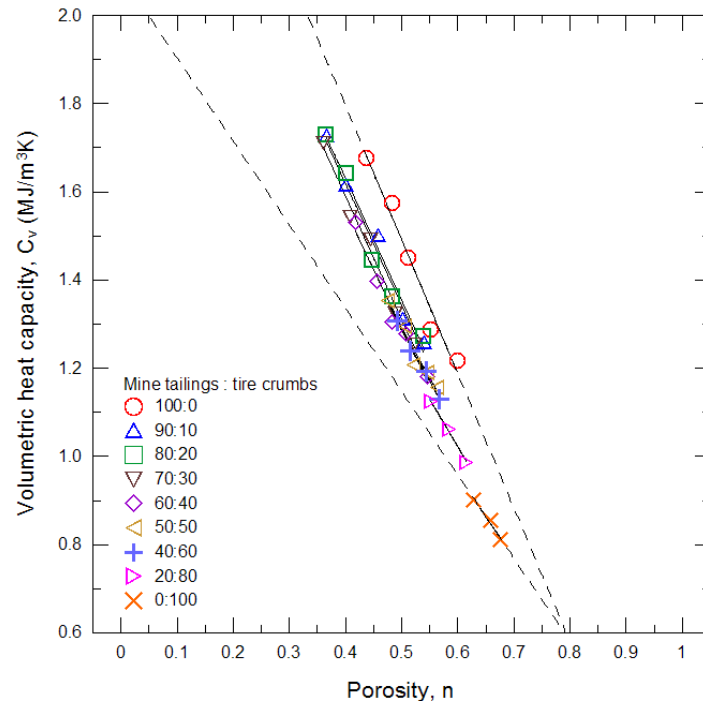
1  
2  
3

Fig. 10 Effect of weight mixing ratio of mine tailings and tire crumbs mixtures on thermal conductivity



4  
5

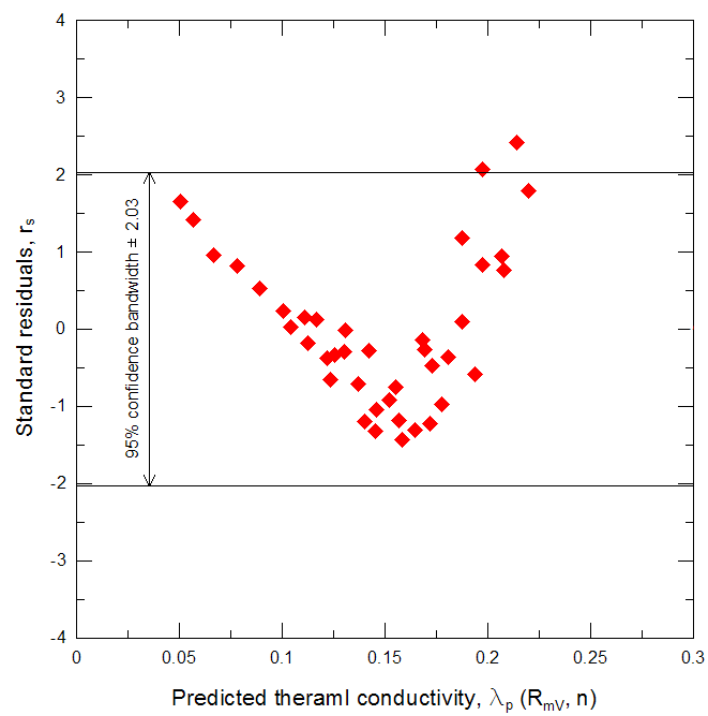
Fig. 11 Thermal conductivity of various dry geomaterials



1

2 Fig. 12 Effect of weight mixing ratio of mine tailings and tire crumbs mixtures on volumetric heat  
 3 capacity

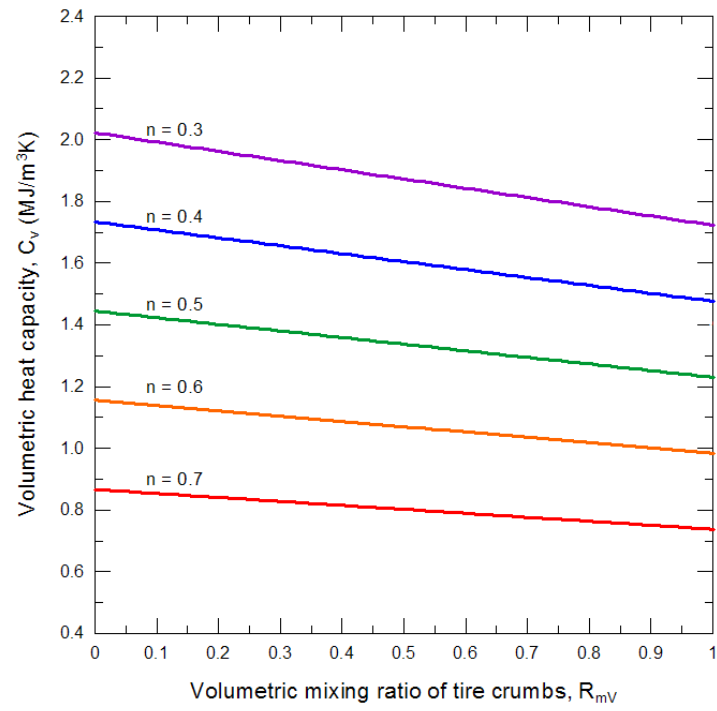
4



5

6

Fig. 13 Standard residuals of a regression model with two variables



1

2 Fig. 14 Change of volumetric heat capacity at different volumetric mixing ratios of tire crumbs and  
3 porosities

4